Specialized eRpL22 paralogue-specific ribosomes regulate specific mRNA translation in spermatogenesis in *Drosophila melanogaster*

Catherine M. Mageeney and Vassie C. Ware*
Department of Biological Sciences, Lehigh University, Bethlehem, PA 18015

ABSTRACT **The functional significance of ribosome heterogeneity in development and differentiation is relatively unexplored. We present the first in vivo evidence of ribosome heterogeneity playing a role in specific mRNA translation in a multicellular eukaryote. Eukaryotic-specific ribosomal protein paralogues eRpL22 and eRpL22-like are essential in development and required for sperm maturation and fertility in *Drosophila*. eRpL22 and eRpL22-like roles in spermatogenesis are not completely interchangeable. Flies depleted of eRpL22 and rescued by eRpL22-like overexpression have reduced fertility, confirming that eRpL22-like cannot substitute fully for eRpL22 function, and that paralogues have functionally distinct roles, not yet defined. We investigated the hypothesis that specific RNAs differentially associate with eRpL22 or eRpL22-like ribosomes, thereby establishing distinct ribosomal roles. RNA-seq identified 12,051 transcripts (mRNAs/noncoding RNAs) with 50% being enriched on specific polysome types. Analysis of ~10% of the most abundant mRNAs suggests ribosome specialization for translating groups of mRNAs expressed at specific stages of spermatogenesis. Further, we show enrichment of "model" eRpL22-like polysome-associated testis mRNAs can occur outside the germline within S2 cells transfected with eRpL22-like, indicating that germline-specific factors are not required for selective translation. This study reveals specialized roles in translation for eRpL22 and eRpL22-like ribosomes in germline differentiation.**

Monitoring Editor
A. Gregory Matera
University of North Carolina

Received: Feb 4, 2019
Revised: Jun 3, 2019
Accepted: Jun 7, 2019

INTRODUCTION

Ribosomes have classically been viewed as static, homogeneous molecular machines capable of indiscriminate translation of the entire population of mRNAs within a cell. Recent evidence suggests this generalization is more complex and that variable composition of ribosomes adds a regulatory feature to translation, likely as a function of physiological or developmental states (reviewed by Xue and Barna, 2012; Shi and Barna, 2015; Genuth and Barna, 2018). Although hypotheses have existed for more than 40 years, suggesting that heterogeneous populations of ribosomes exist and may be involved in developmental regulation (reviewed in Ramagopal, 1992; Mauro and Edelman, 2002), the functional significance of ribosome heterogeneity is just beginning to unfold.

While a generic eukaryotic ribosome contains four rRNAs and 79 ribosomal proteins (Rps; Warner, 1999; Ben-Shem *et al.*, 2011), many eukaryotic genomes encode more Rps than are assembled into a ribosome. Genome or gene duplication events during

This article was published online ahead of print in MBoC in Press (http://www.molbiolcell.org/cgi/doi/10.1091/mbc.E19-02-0086) on June 12, 2019.

C.M.M. and V.C.W. conceptualized the study; C.M.M. and V.C.W. developed the methodology; C.M.M. collected the data; C.M.M. and V.C.W. analyzed and interpreted the data; C.M.M. and V.C.W. wrote the original draft and reviewed and edited the manuscript; V.C.W. was responsible for funding acquisition.

*Address correspondence to: Vassie C. Ware (vcw0@lehigh.edu).

Abbreviations used: ACXA, adenylyl cyclase X A; can, cannonball; Fadd, Fas-associated death domain; FC, fold change; FDRs, false discovery rates; GEO, Gene Expression Omnibus; glob3, globin 3; GO, Gene Ontology; IHC, immunohistochemistry; IP, immunoprecipitation; lncRNAs, long noncoding RNAs; Marf, mitochondrial assembly regulatory factor; MCTS1, malignant T-cell amplified sequence 1; mESCs, mouse embryonic stem cells; mtRNAs, mitochondrial RNAs; ncRNAs, noncoding RNAs; NFDM, nonfat dry milk; NTC, no template control; PBS, phosphate-buffered saline; PTM, posttranslational modification; *r*-cup, Ryder-cup; RAPs, ribosome-associated proteins; RNA-seq, RNA sequencing; Rp, ribosomal protein; S2, Schneider 2; sd-RNAs, small nucleolar RNA-derived small RNAs; Shal, Shaker cognate l; snoRNAs, small nucleolar RNAs; stil, stand still; TAE, Tris acetate-EDTA; Taf1, TBP-associated factor 1; TBP, TATA-binding protein; TIMP, tissue inhibitor of metalloproteases; UTR, untranslated region; WT, wild type.

evolution account for the existence of Rp paralogues in many organisms. Assembly of different Rp paralogues into ribosomes increases the complexity of ribosomal composition and raises the possibility of functional differences between ribosomes based on specific paralogue content as proposed by Komili *et al*. (2007) in describing the "ribosome code" (reviewed by Gerst, 2018). Expression of paralogous Rp genes raises several important questions: are Rp paralogues functionally redundant within the ribosomal pathway or alternatively, have these proteins evolved novel roles which may include extraribosomal roles (reviewed by Wool, 1996; Warner and McIntosh, 2009)? Within the ribosomal pathway, are paralogue-specific ribosomes functionally specialized with a capacity for differential translation of specific mRNAs?

Evidence for the existence of "specialized ribosomes" is accumulating from several recent studies. Kondrashov *et al*. (2011) showed that genetic depletion of eukaryotic-specific core RP eRpL38 results in reduced translation of a subset of *hox* mRNAs and defects in establishment of the mammalian body plan, suggesting that ribosomes containing core eRpL38 are specialized in development for translation of this class of mRNAs. Several mass spectrometry studies (e.g., Slavov *et al*., 2015; Shi *et al*., 2017) show further support for the specialized ribosome hypothesis, demonstrating that stoichiometric differences in core Rps generate distinct ribosome populations with distinct physiological functions. eRpS25-specific and uRpL10-specific ribosomes in mouse embryonic stem cells (mESCs) preferentially translate different subsets of transcripts involved in specific metabolic or cellular pathways (Shi *et al*., 2017).

Studies of ribosome heterogeneity, generated by differential assembly of Rp paralogues, offer further insights into the specialized ribosome hypothesis. A recent study in yeast determined that depletion of structurally identical Rp paralogues RPL1b and RPL1a results in mitochondrial protein deficiencies (Segev and Gerst, 2018). Although this study provides important insights into translational specificity for paralogue-specific ribosomes in yeast, it remains unclear whether differential functions of paralogue-specific ribosomes affect cell or tissue differentiation and development in multicellular eukaryotes. For these studies, we have explored the functional significance of ribosomes that differ in paralogue content within the male germline in *Drosophila melanogaster*.

Several duplicated Rp genes in the fly show tissue-specific expression, but RpS5b, RpS19b, RpL10Aa, RpL37b, RpS28-like, and eRpL22-like show testis-specific expression (Marygold *et al*., 2007). From this group, the eRpL22 family provides an excellent system to explore questions about the impact of ribosome heterogeneity in a developmental context and to explore the specialized ribosome hypothesis.

The *eRpL22* gene family consists of two members: ancestral *erpL22* and the duplicated *erpL22-like* (identified by Kai *et al*., 2005). In *Drosophila* both proteins are essential for development and importantly for this study, are required for sperm production and fertility (Mageeney *et al*., 2018). eRpL22 and eRpL22-like functions in spermatogenesis are not completely redundant, as paralogue depletion and partial rescue studies demonstrate that paralogues have unique roles as well (Mageeney *et al*., 2018).

eRpL22 and eRpL22-like share 38% amino acid identity (Marygold *et al*., 2007) with considerable conservation in the C-terminal rRNA-binding domain. Each protein contains an N-terminal extension with extensive homology to the C-terminal domain of histone H1 (Koyama *et al*., 1999; Kearse *et al*., 2011), unlike eRpL22 orthologues described in other eukaryotic species. In addition to structural differences, eRpL22 paralogues are differentially expressed. eRpL22 is expressed ubiquitously in adult flies (Shigenobu *et al*., 2006a,b; Crosby *et al*., 2007; Kearse *et al*., 2011), while eRpL22-like has tissue-specific expression in adult heads with highest levels found in the adult male germline (Kearse *et al*., 2011). Both paralogues are coexpressed in the male germline and undergo differential posttranslational modification (PTM) in germ cells (Kearse *et al*., 2013; Mageeney and Ware, unpublished). In germline stem cells and mitotic spermatocytes, eRpL22 is localized in the cytoplasm and nucleolus (typical of a ribosomal protein). However, in later stages of spermatogenesis, eRpL22 has a nuclear distribution with a punctate pattern in the nucleoplasm as meiotic progression proceeds (Kearse *et al*., 2013). eRpL22-like accumulates in the cytoplasm in all stages of spermatogenesis (Kearse *et al*., 2013), consistent with an active ribosomal role and corroborated by Kearse *et al*. (2013). Both proteins are components of actively translating ribosomes in the fly (Kearse *et al*., 2011).

For eRpL22, several factors may affect its assembly into ribosomes during sperm development. eRpL22 undergoes SUMOylation in all tissues, but additional SUMOylation and phosphorylation occurs within the germline lineage, clearly apparent in meiotic spermatocytes (Kearse *et al*., 2013). SUMOylated eRpL22 is not a component of actively translating ribosomes (Kearse *et al*., 2013). The change in eRpL22 subcellular localization from the cytoplasm into the nucleus during meiotic stages of spermatogenesis may also reduce its availability for the Rp pathway during later stages of spermatogenesis.

This study uncovers a population of eRpL22 paralogue-specific specialized ribosomes in the fly testis which may define distinct roles implicated for eRpL22 paralogues in spermatogenesis from a previous study (Mageeney *et al*., 2018). Wild-type testes were used to isolate eRpL22 paralogue-specific ribosomes (denotes inclusion of both ribosome types) complexed with RNA molecules. RNA sequencing determined the distribution of RNAs on each type of eRpL22 paralogue-specific ribosome, revealing unique translatomes for both eRpL22- and eRpL22-like ribosomes, as well as an overlapping translatome. Analysis of ~10% of RNAs in the complete data set (inclusive of most abundant RNAs with lowest variations in normalization value and significant p values) shows that eRpL22 ribosomes predominately translate early testis-specific and ubiquitously expressed mRNAs, while eRpL22-like ribosomes primarily translate testis-specific transcripts or transcripts not previously investigated. Noncoding RNAs (ncRNAs) with unknown roles were identified in association with each ribosome type. Altogether, these data provide additional evidence for specialized ribosomes distinguished by different associated RNAs and different translatomes. This is the first known characterization of specialized ribosomes with translational specificity within a cellular differentiation pathway in a multicellular eukaryote.

RESULTS

Immunoprecipitation with paralogue-specific antibodies isolates homogeneous populations of polysomes from the testis

The process of spermatogenesis (reviewed by Fuller, 1993) is well studied as a model for investigating cellular and molecular mechanisms specifying cellular differentiation. The process is initiated within the stem cell hub and proceeds in tightly regulated stages with stage-specific protein requirements to produce mature sperm. Both transcriptional and translational control mechanisms are widely known to impact the production of the proteome at specific stages of spermatogenesis (e.g., White-Cooper, 2010; Lim *et al*., 2012; Fuller, 2016). Testis-specific transcription before and after meiosis has been widely studied (reviewed by White-Cooper, 2010). Translation

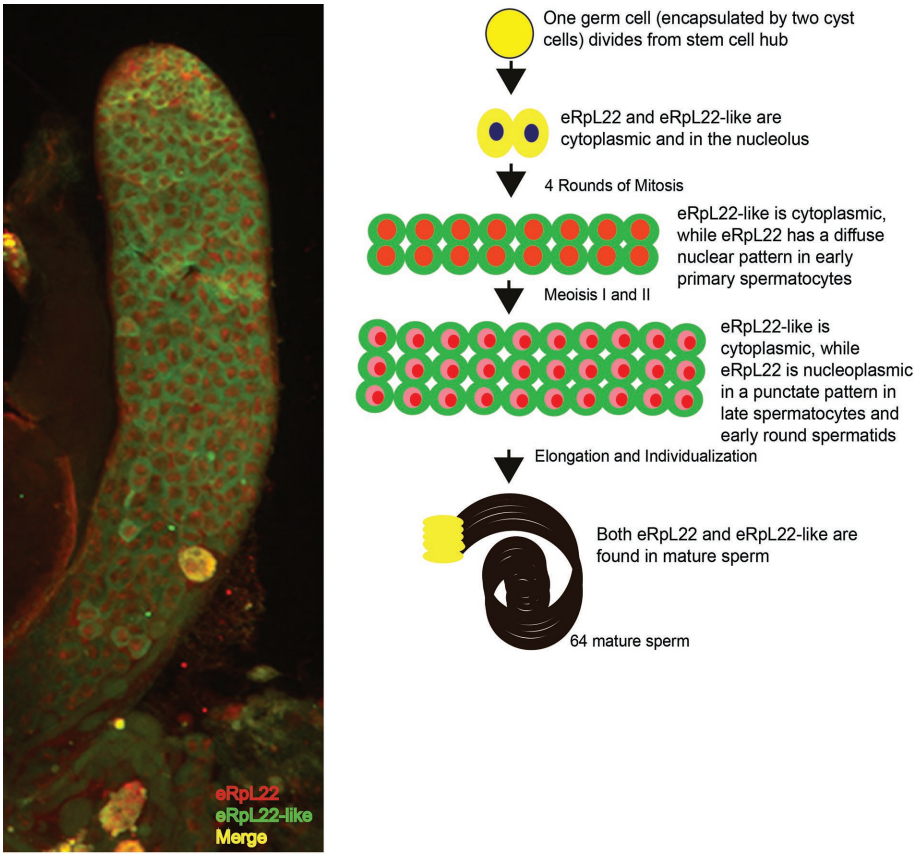

FIGURE 1: *Drosophila* spermatogenesis diagram with localization of eRpL22 paralogues. Left, IHC image of wild-type *Drosophila* testis. eRpL22 (red) and eRpL22-like (green). Right, schematic showing eRpL22 paralogue localization during spermatogenesis (eRpL22 [red] and eRpL22-like [green]). In early stages of spermatogenesis eRpL22 and eRpL22-like are colocalized in the cytoplasm and nucleolus. As spermatogenesis progresses into meiosis eRpL22 becomes localized to the nucleus in a diffuse pattern and then becomes nucleoplasmic with a punctate pattern, while eRpL22-like remains in the cytoplasm. Mature sperm contain both eRpL22 and eRpL22-like.

of several transcripts, synthesized at earlier stages of spermatogenesis and stored as translationally inert ribonucleoproteins, is delayed until later stages of spermatogenesis, through translational control mechanisms not completely understood (e.g., reviewed by Schäfer *et al.*, 1995; Hempel *et al.*, 2006; Baker *et al.*, 2015, Ghosh and Lasko, 2015). The extent to which ribosome heterogeneity, defined by differences in RP paralogue content, contributes to translational control mechanisms that regulate the spatial and temporal production of specific proteins required for spermatogenesis is unknown.

Our approach was to determine RNA content of actively translating testis ribosomes isolated from polysome profiles using eRpL22- or eRpL22-like–specific antibodies for affinity purification. Paralogue-specific antibodies were previously used in initial expression studies (Kearse *et al.*, 2011) to demonstrate coexpression of eRpL22 paralogues in germ cells during *D. melanogaster* spermatogenesis (Figure 1; Kearse *et al.*, 2011, 2013). Because immunohistochemical (IHC) staining previously showed a pattern of expression for eRpL22 and eRpL22-like in germ cells at all stages of spermatogenesis (Kearse *et al.*, 2013), we expected our immunoprecipitation strategy to capture paralogue-specific polysomes from all spermatogenesis stages because cytoplasmic staining is evident from the spermatogonial stage to the spermatid stage. A change in subcellular distribution of eRpL22, as it occurs within meiotic spermatocytes from the cytoplasm to the nucleoplasm (Kearse *et al.*, 2013), would be expected to change the proportion of eRpL22 within the active ribosome pool, affecting the quantity of eRpL22 ribosomes compared with eRpL22-like ribosomes captured from this stage. Additionally, we predicted that RNAs from both somatic and germline cell lineages would be represented in the testis RNA-seq pool.

Four replicates of ribosomal profiles from testes were fractionated and analyzed by Western blot (using antibodies specific for eRpL22 or eRpL22-like) to score sedimentation of specific paralogue complexes across 10–50% linear sucrose gradients, with a particular interest in sedimentation of paralogues with the active translation machinery (Supplemental Figure 1, A–E). eRpL22 and eRpL22-like paralogues display differential sedimentation within fractionated polysome profiles (Figure 2A and Supplemental Figure 1E). Sedimentation of eRpL22-like across the gradient suggests its inclusion in other types of complexes distinct from intact 60S ribosomal subunits or 80S monosomes within germ cells.

To pursue isolation of populations of RNAs found in association with polysomes containing either eRpL22 or eRpL22-like, we first used paralogue-specific antibodies (antibody epitope: Kearse *et al.*, 2011) to capture specific polysome types by immunoprecipitation (IP) from pooled polysome fractions from each of four ribosome gradients. Western blot analysis confirmed that an eRpL22 IP from pooled polysome fractions pulled down eRpL22 ribosomes, but not eRpL22-like ribosomes (Figure 2B). In reciprocal IPs using specific eRpL22-like antibodies, eRpL22-like was captured from testis polysome fractions without also pulling down eRpL22 ribosomes, as shown by the absence of detectable eRpL22 from eRpL22-like IPs (Figure 2C). Lack of detection of the opposing paralogue from a specific IP is suggestive that polysomes are not mixed paralogue populations; captured polysomes appear to contain only one paralogue type—either eRpL22 or eRpL22-like. This observation may shape proposals for how paralogue-specific 60S subunits form initiation complexes with mRNAs and the 40S subunit to initiate translation.

Translatome profiling reveals overlapping and distinct populations of mRNAs in association with eRpL22- or eRpL22-like polysomes from testes

Total RNA from eRpL22 paralogue-specific polysome fractions was analyzed by RNA sequencing. FASTQ files were trimmed and mapped to the r6v15 version of the *D. melanogaster* genome. From eRpL22 paralogue-specific polysome IPs, 12,051 transcripts were identified from among four replicates of pooled polysome fractions for each paralogue IP. One eRpL22-specific replicate was removed from analysis due to low data output. Fold-change (FC) differences in mRNA association were calculated by averaging normalization values for eRpL22 polysome replicates and eRpL22-like polysome replicates and then dividing the log2 of eRpL22-like polysomes by eRpL22 polysomes. Analysis of RNA

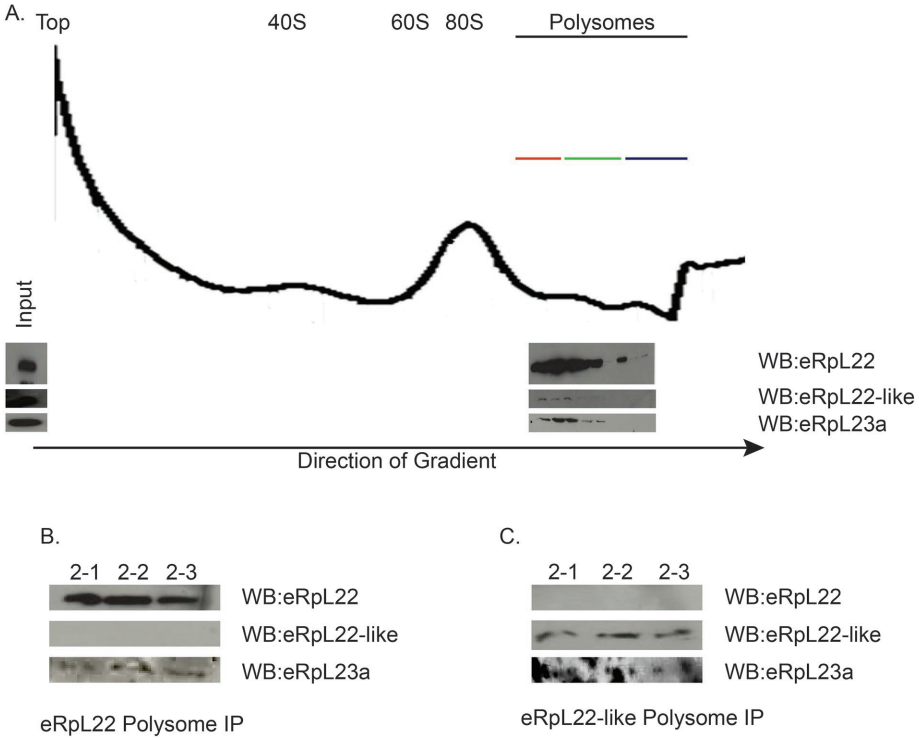

FIGURE 2: eRpL22 paralogue-specific ribosomes can be immunopurified from *D. melanogaster* testis polysomes. (A) Ribosomal profile gradient from 2000 testis pairs. The top of the gradient, 40S, 60S, 80S, and polysomes are denoted. Western blot analysis shows eRpL22 cosediments with polysomes. eRpL23a is found in polysomes, coincident with the eRpL22 signal. The line indicates the fractions (red: 2-1, green: 2-2, and purple: 2-3) that were used for polysome pools, IP and RNA-seq. Traces for all four replicates are shown in Supplemental Figure 1. (B) eRpL22 IP shows eRpL22 polysomes can be isolated without eRpL22-like isolation. eRpL23a is observed in each fraction, indicative of the presence of this essential Rp in polysomes. Note the antibody used for eRpL22 Western blot analysis here and in C for these experiments is different from that used in Kearse *et al.* (2011, 2013) and does not detect higher molecular weight species of eRpL22, which is not a component of polysomes (Kearse *et al.*, 2013). (C) eRpL22-like IP shows eRpL22-like polysomes can be isolated without eRpL22 isolation. Samples 2-1, 2-2, 2-3 are three pools of polysome fractions divided between three IP isolates. eRpL23a is present in each fraction. RNA from these isolates was combined in equal concentrations for RNA sequencing.

distribution on paralogue-specific polysomes revealed that ~50% (6073) of transcripts were found equally associated with both polysome types, with no apparent FC differences (Figure 3A). Notably, the remaining 50% of mRNAs were associated with a particular polysome type, indicating unique translatomes for each polysome type as well. Approximately 22% (2613) of mRNAs were associated with eRpL22 polysomes with the remaining 28% (3365) of mRNAs found enriched on eRpL22-like polysomes (Figure 3A).

More detailed analyses were performed on ~10% of transcripts found in greatest abundance (based on most statistically significant *p* values <0.07) in the data set. Within this group, we could identify several transcripts with known temporal expression patterns in spermatogenesis such as transcripts expressed during meiosis or in later stages of spermatogenesis, or those defined as testis-specific or ubiquitously expressed. Complete analysis of the entire RNA-seq data set will be forthcoming to determine what, if any, conserved features may be evident among transcripts enriched on each paralogue-specific ribosome type.

A heat map, constructed to show the top 40 transcripts (sorted by *p* value, regardless of paralogue-specific polysome type) shows that replicates were generally consistent (Figure 3, B and C). Transcripts found enriched on eRpL22-like polysomes were enriched in nearly all replicates and the same is true for those enriched on eRpL22 polysomes (Figure 3, B and C). Additionally, transcripts that are enriched on eRpL22-like polysomes generally appear to be depleted from eRpL22 polysomes in this subset of transcripts (Figure 3, B and C). Collectively, these data support the hypothesis that subpopulations of mRNAs are translated on specific polysome types distinguished by eRpL22 paralogue content.

RT-PCR was used to confirm the integrity of several mRNAs as well as the pattern of association with specific polysome types. RT-PCR products representing mRNA transcripts were derived from internal primer sets that hybridize to internal regions of respective transcripts. In addition, RT-PCR analysis replicated RNA-sequencing results for a selected number of transcripts found in association with specific polysome types. Both *erpL22* (FC: −1.1) and *erpL22-like* (FC: −1.2) mRNAs were found through RT-PCR analysis on both polysome types, mirroring RNA-sequencing results (Supplemental Figure 2, A and B, respectively). *traffic jam* (FC: −2.45) mRNA, a marker for somatic cyst cells in the testis (Li *et al.*, 2003), was found associated with eRpL22 polysomes, as expected (Supplemental Figure 2C).

Gene Ontology (GO) analysis (Ashburner *et al.*, 2000; GO Consortium, 2017; Mi *et al.*, 2017) was used to determine whether mRNAs from particular biological processes were enriched on either eRpL22 paralogue-specific ribosome type using false discovery rates (FDRs) of <0.05. The GO terms are not particularly informative to identify the types of spermatogenesis transcripts associated on each paralogue-specific polysome type (Table 1). However, GO terms did reveal that certain mRNAs associated with cytoplasmic translation are found enriched on specific polysome types. Transcripts enriched on eRpL22 polysomes were eRpL22, eRpL22-like, and malignant T-cell amplified sequence 1 (MCTS1), a noncanonical translation initiation factor that promotes translation reinitiation (FC: −2). mRNAs for two methyltransferases (CG7009 and CG5220), RpLP0-like, and RpS10a were found on eRpL22-like polysomes. While the GO analysis indicates no preference for spermatogenesis transcripts on eRpL22-like polysomes, it should be noted that many transcripts found on eRpL22-like ribosomes either have no previously annotated functions or encode protein products detected in large mass spectrometry experiments (Dorus *et al.*, 2006; Wasbrough *et al.*, 2010). Individual analyses of all transcripts from these data sets show that many late-stage spermatogenesis transcripts are found in association with eRpL22-like ribosomes. GO analysis with FDR >0.05 reveals that numerous transcripts associated with eRpL22-like polysomes are involved in various stages of spermatogenesis and meiosis.

Further investigation into known spermatogenesis transcripts shows many testis-specific transcripts are not preferentially associated with either polysome type; however, many of these transcripts

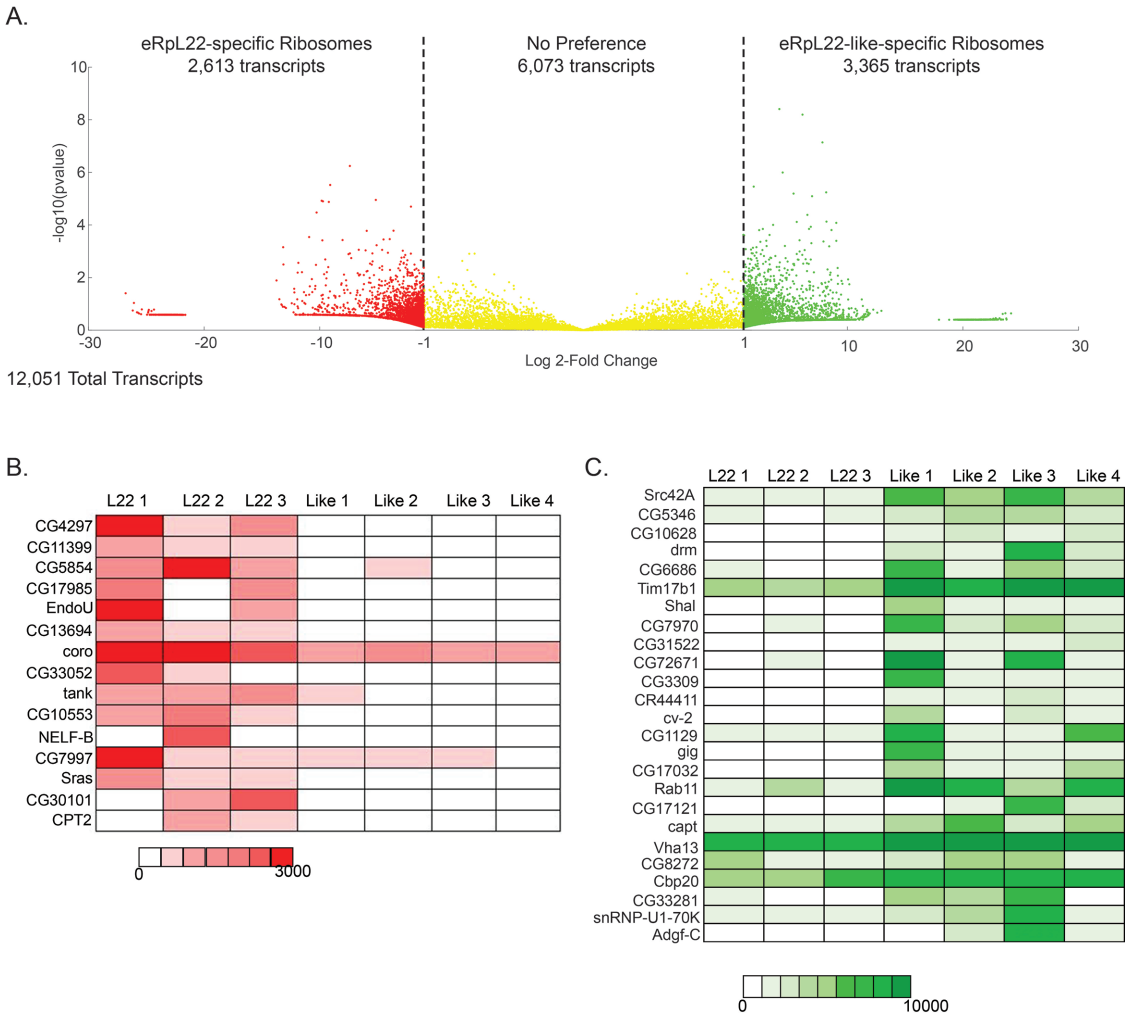

FIGURE 3: eRpL22 paralogue-specific testis polysomes are enriched for unique mRNAs. (A) Volcano plot showing transcripts enriched on eRpL22 polysomes (red), eRpL22-like polysomes (green), and those mRNAs with no preference for either eRpL22 paralogue-specific polysome (yellow). The volcano plot depicts the significance (–log10[*p* value]) vs. the fold change (log2-fold change). The number of transcripts found on each type of ribosome is listed. One transcript, Src42A, is not shown in this scale (–log10[*p* value]:17.24, FC: 3.97). (B) Heat map of select group of RNAs enriched on eRpL22 polysomes found in the top 40 of total transcripts. Note that transcripts enriched on eRpL22 polysomes are depleted on eRpL22-like polysomes. The replicate number for each IP is indicated following L22 for eRpL22 or Like for eRpL22-like. (C) Heat map of RNAs enriched on eRpL22-like polysomes found in the top 40 total transcripts. Transcripts enriched on eRpL22-like polysomes are depleted on eRpL22 polysomes. Heat map units are normalized read counts.

have very low *p* values (Supplemental Table 1). This result may not be unexpected because most testis-specific transcripts are transcribed in primary spermatocytes, stored, and then translated during spermatid elongation (reviewed by Schäfer *et al.*, 1995). This group of transcripts may be underrepresented on polysomes in these samples. A few transcripts, shown to be expressed early in spermatogenesis and translationally repressed until meiosis or thereafter, had no preferred association with either paralogue-specific polysome type. Cyclin B (FC: –0.163), previously shown by Baker *et al.* (2015) to be transcribed during mitosis at the apical tip and then its mRNA translationally repressed in immature and growing spermatocytes, is within this group.

Another class of spermatogenesis-specific genes found in our data set were the *comet* and *cup* genes. The *comet* and *cup* genes are a group of 24 genes detected at low levels during spermatogenesis (through mitosis, meiosis, and early spermatid elongation) but are up-regulated during later stages of spermatid elongation (Barreau *et al.*, 2008). The majority of transcripts for these genes (20/24) were found in our data set. Sixteen of twenty-four (~67%) were found on both eRpL22 paralogue-specific ribosome types with no preference. *Ryder-cup* (*r-cup*) was found on eRpL22-like polysomes (FC: 1.2). Transcripts for a few *cup* genes were enriched on eRpL22 polysomes (*david-cup* [FC: –1.2]; *stanley-cup* [FC: –3.15]; *flyers-cup* [FC: –1.2]). This is an important exception to the general rule that late-stage testis-specific transcripts associate with eRpL22-like polysomes and demonstrates that a population of eRpL22 polysomes functions in postmeiotic elongating sperm after the major shift in subcellular distribution of eRpL22 from the cytoplasm to the nucleoplasm in meiotic spermatocytes (Kearse *et al.*, 2013).

Many transcripts (found in other data sets of proteins and mRNAs expressed in sperm; Wasbrough *et al.*, 2010; Fisher *et al.*, 2012) required for spermatogenesis have no association preference for either polysome type. However, transcripts (such as globin 3 [glob3; FC: 2.1; FBgn0037385], Fas-associated death domain [Fadd; FC:

GO biological process	Number of transcripts	% of Reference	*p* Value
eRpL22 polysomes			
Animal Organ Development	252	20.8	6.56e-05
Anatomical Structure Morphogenesis	318	20	8.05e-05
Regulation of Cellular Process	636	18.6	1.77e-05
ATP metabolic process	4	2.8	6.58e-06
eRpL22-like polysomes			
Transport	447	25.4	2.36e-05
Regulation of Cellular Process	813	23.9	1.15e-05
Cytoplasmic Translation	4	3.6	1.42e-05
No preference			
Mitochondrial Electron Transport, NADH to Ubiquinone	35	94.6	3.42e-04
Cytoplasmic Translation	102	92.7	1.47e-09
Sperm Individualization	41	83.7	6.18e-04
Protein Targeting to Mitochondria	41	83.7	6.18e-04

Transcripts found in association with each eRpL22 paralogue-specific ribosome and transcripts with no preference were submitted to the GO ontology enrichment tool (Ashburner *et al.*, 2000; GO Consortium, 2017; Mi *et al.*, 2017) to determine whether any biological processes were enriched in each class. FDR < 0.05.

TABLE 1: GO ontology analysis of eRpL22 paralogue-specific translatomes.

3.8; FBgn0038928], and adenylyl cyclase X A (ACXA; FC: 1.6; FBgn0040510]) associated with eRpL22-like polysomes appear to be those required during meiosis and in later stages of spermatogenesis. Transcripts required earlier during the mitotic phase of spermatogenesis in spermatogonia are typically found on both types or specifically on eRpL22 polysomes. Testis-specific transcripts found in association with eRpL22 polysomes include TBP-associated factor [Taf1] (FC-3; FBgn0010355), mitochondrial assembly regulatory factor (Marf) (FC: −1.6; FBgn0029870), and stand still (stil) (FC: -1.1; FBgn0003527). The mechanism by which a specific mRNA, coupled with a 40S small ribosomal subunit initiation complex, is targeted to a 60S large ribosomal subunit, assembled with either eRpL22 or eRpL22-like, remains unknown.

Numerous ncRNAs associate with eRpL22 paralogue-specific ribosomes

Of the subpopulations of RNAs found in association with paralogue-specific polysomes, ncRNAs comprise 11% (1366) of the total RNAs captured (Supplemental Figure 3A). Assessment of the distribution of ncRNAs shows an equal distribution of these RNAs across each ribosome type. The number of ncRNAs associated with eRpL22-like polysomes is slightly larger than for ncRNAs found in association with eRpL22 ribosomes or for ncRNAs that associate with both polysome types (Supplemental Figure 3B).

Different classes of ncRNAs are enriched on each polysome type. Functions of the majority of *Drosophila* ncRNAs are understudied and most ncRNAs have not as yet been assigned a "class" designation. Mitochondrial RNAs (mtRNAs) are the most abundant class found in association with eRpL22 polysomes (Supplemental Figure 3C). Mitochondrial RNA accumulation within the cytoplasm offers several intriguing possibilities for linking mitochondrial and cytoplasmic processes. Small nucleolar RNAs (snoRNAs) are the most abundant ncRNA found in association with eRpL22-like polysomes (Supplemental Figure 3D). Pseudogene ncRNAs were the most abundant class of ncRNAs found with no association preference for either polysome type. It is noteworthy that pseudogene rRNAs are also found in this data set. All but one are found in association with both polysome types and some pseudogene rRNAs are similar in size to canonical rRNAs (Table 2). It is interesting to speculate that assembly of pseudogene rRNAs into paralogue-specific ribosomes would create additional levels of ribosome heterogeneity and specialized ribosomes within the testis.

Recent studies implicate ncRNAs in translational regulation (reviewed by Pircher *et al.*, 2014; Wen *et al.*, 2016). Many long noncoding RNAs (lncRNAs) described in those studies also associate with specific polysome types. Thirty-five percent (25/71) of lncRNAs described by Wen *et al.* (2016) are found on eRpL22-like polysomes while 48% (34/71) displayed no association preference (specific RNAs and distributions found in Supplemental Table 1). It is therefore conceivable that ncRNAs associating with eRpL22 paralogue-specific polysomes are involved in translational regulation during spermatogenesis.

We have recently uncovered a unique mechanism of cross-talk regulation between eRpL22 paralogues, suggesting negative regulation of eRpL22 by eRpL22-like (Mageeney *et al.*, 2018). Depletion of eRpL22-like by testis-specific RNAi-mediated strategies resulted in increases in both *erpL22* mRNA (shown by qRT-PCR) and eRpL22 protein levels (shown by Western blot). Depletion of eRpL22, however, did not result in an increase in eRpL22-like levels; instead, eRpL22-like levels were diminished. What factors control paralogue levels within the germline are unknown; yet, posttranscriptional mechanisms, more complex than compensatory processes designed for overall equilibration of paralogue stoichiometry, should be considered as possibilities.

Our RNA-seq data suggest an intriguing hypothesis that may address cross-talk mechanisms between eRpL22 and eRpL22-like to regulate paralogue levels. Four ncRNAs (encoded near or within the *erpL22* locus), identified in this study, are of interest: lncRNA44965 (encoded in reverse, 115 base pairs downstream from the *erpL22* termination site), lncRNA42491 (encoded within the *erpL22* coding region), and snoRNAs, Psi28S:2179 and Psi18S-531(both encoded within the second *erpL22* intron; Supplemental Figure 3E). Molecular functions of these ncRNAs are unknown. These ncRNAs,

RNA name	Length (nt)	Fold change (ribosome association)
18SrRNA-Psi:CR41602	**1975**	**–0.16455 (no preference)**
28SrRNA-Psi:CR40741	1258	−0.73389 (no preference)
28SrRNA-PSI:CR41609	895	−0.65948 (no preference)
28SrRNA-Psi:CR45853	255	−2.76489 (eRpL22-specific)
28SrRNA-Psi:CR45855	704	−0.32199 (no preference)
28SrRNA-Psi:CR45859	**2689**	**–0.49392 (no preference)**
28SrRNA-Psi:CR45860	357	−0.57154 (no preference)
5.8SrRNA:Psi-CR45863	123	−0.31443 (no preference)

Pseudogenes rRNA were found in association with eRpL22 paralogue-specific ribosomes. Fold change expressed as a negative number has more transcripts associated with eRpL22 polysomes than eRpL22-like polysomes. Assessment of the length of pseudogenes rRNA may reveal information about incorporation into ribosomes. Those in bold have sizes similar to the canonical rRNA lengths. Canonical rRNA molecules length: 18S (1995 nt), 5.8S (123 nt), 2S (30 nt), and 28S (3945 nt) (Tautz *et al.*, 1988).

TABLE 2: Pseudogenes rRNA found in association with eRpL22 paralogue-specific ribosomes.

except the snoRNA Psi28S:2179, were found in association with eRpL22-like ribosomes. ncRNA snoRNA:Psi28S:2179 was absent from this data set, suggesting it is either not stably expressed in the testis, is not stably associated with eRpL22 paralogue-specific ribosomes, or is compartmentalized elsewhere outside the ribosomal pool. ncRNAs encoded from the *erpL22* gene locus may have a role in an eRpL22–eRpL22-like cross-talk mechanism that regulates *erpL22* mRNA translation or *erpL22* mRNA stability, mediated through associations with eRpL22-like ribosomes.

mRNAs enriched on eRpL22-like ribosomes in the testis are preferentially loaded onto eRpL22-like ribosomes in transfected S2 cells independent of testis-specific factors

To begin investigations into mechanisms that contribute to preferential entry of mRNAs onto specific ribosome types, we asked whether germ cell–specific factors are required for mRNA enrichment. Two transcripts (identified by RNA-seq) were selected for heterologous expression within S2 cell lines. Shaker cognate I (Shal; FC: 8.2; FBgn0005564) and tissue inhibitor of metalloproteases (TIMP; FC: 6.9; FBgn0025879) were selected because of a high fold-change association difference on eRpL22-like polysomes in the testis, statistically significant *p* values, little or no association with eRpL22 polysome replicates, no documented expression in S2 cells, and the availability of antibodies to assess protein accumulation.

As a prelude to Shal and TIMP studies in S2 cells, we investigated expression of these genes within the testis. As a voltage-dependent A-type K^+ channel (FlyBase.org), Shal protein expression has been studied primarily in the nervous system. Although not detectable in whole testes extracts, Shal protein was detected in mature sperm captured from seminal vesicles, as shown by Western blot analysis (Figure 4A). To determine the stage in which *shal* mRNA is expressed in the testis, a spermatogenesis meiotic-arrest mutant was used. Spermatogenesis in *cannonball* (*can*) mutants is arrested at the G2/M transition of meiosis I, resulting in the absence of postmeiotic spermatocytes (Lin *et al.*, 1996). RT-PCR experiments using mRNA from *can* mutant testes revealed the presence of some *shal* mRNA, suggesting that *shal* mRNA is transcribed before the completion of meiosis (Figure 4B). Thus, there is likely a temporal gap between *shal* mRNA transcription at a stage before meiosis and the accumulation of Shal protein in later stages of spermatogenesis after meiosis, based on these analyses.

TIMP expression has also been studied primarily in the nervous system and the wing (FlyBase.org). Western blot analysis of whole testis tissue revealed TIMP protein in adult testes (Figure 4C) and RT-PCR analysis showed *timp* mRNA in *can* mutant testes, both suggesting *timp* is expressed before the completion of meiosis (Figure 4D). In fact, IHC analysis confirmed TIMP protein expression throughout spermatogenesis and its localization in the male germline (but not in somatic cyst cells) as shown for eRpL22-like (Figure 4E).

To determine whether *shal* or *timp* mRNAs could be translated on eRpL22 ribosomes or only eRpL22-like ribosomes, S2 cell lines were utilized. Because neither transcript is expressed in S2 cells (previously reported on FlyBase.org and replicated in this study) and S2 cells only express eRpL22 and not eRpL22-like, questions related to specific loading of *shal* and *timp* mRNA onto eRpL22-like ribosomes could be explored.

We used a stable S2 line for inducible expression of plasmid-encoded FLAG–eRpL22-like to determine whether *shal* or *timp* mRNAs are preferentially loaded onto eRpL22-like ribosomes. pMT/*shal* or pMT/*timp* plasmids were transfected into either S2 cells or S2/pMT_FLAG–*erpL22-like* cells (denoted as FLAG–eRpL22-like S2 cells). Both sets of cells were induced on day 0 and at 34 h posttransfection to activate *erpL22-like* expression and either *shal* or *timp* expression. Cell lysates, used for Western blot analysis and IP analyses, were collected 5 d posttransfection (see Supplemental Figure 4 for design). Shal and TIMP (from transfected inducible plasmids) were translated within both S2 and FLAG–eRpL22-like S2 cells (Figure 4, F and G, respectively). FLAG–eRpL22-like was only expressed in FLAG–eRpL22-like S2 cells and no changes in eRpL22 levels were noted (Figure 4, F and G).

To further explore whether *shal* and *timp* mRNAs are preferentially loaded onto eRpL22-like–specific ribosomes in S2 cells, qPCR quantification of mRNAs recovered from eRpL22 and eRpL22-like IPs was performed. As a proxy for mRNA association with paralogue-specific ribosomes, we used paralogue-specific antibodies to pull down eRpL22 paralogues and associated mRNAs in IPs. Relatively more *shal* mRNA was found in association with eRpL22-like ribosomes (compared with eRpL22 ribosomes) in FLAG–eRpL22-like S2 cells (fold change: 4.58; SD: ±0.5). The amount of Shal protein accumulating in both S2 cell lines was comparable (Figure 4F). A comparison of *shal* mRNA levels recovered from eRpL22 IPs in both S2 cell lines showed a reduction in *shal* mRNA associated with eRpL22 ribosomes in FLAG–eRpL22-like S2 cells (fold change: 0.13; SD: ±0.2). Given that a comparable amount of Shal protein accumulates in both cell lines and a reduced amount of *shal* mRNA is found in association with eRpL22 ribosomes within FLAG–eRpL22-like S2 cells, we conclude that *shal* mRNA is preferentially translated on

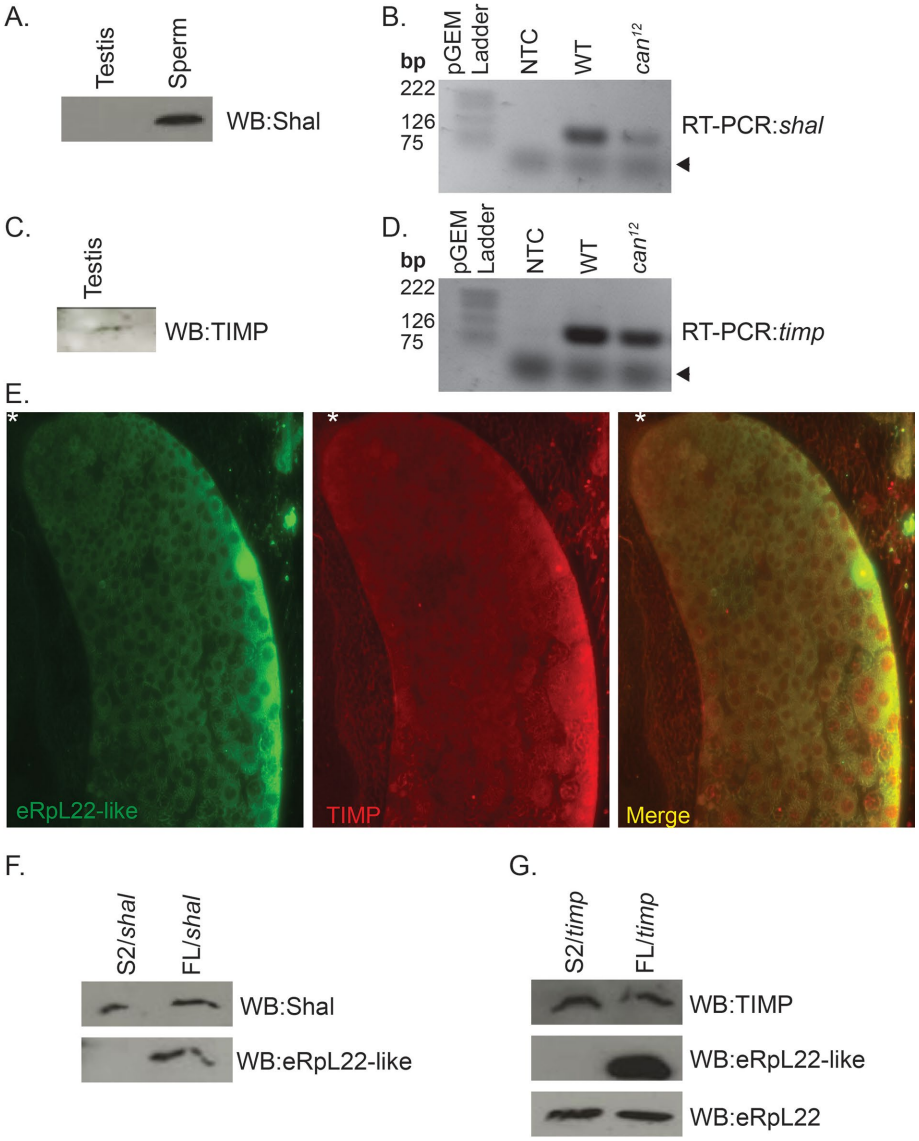

FIGURE 4: Testis mRNAs enriched on eRpL22-like ribosomes are loaded onto both eRpL22- and eRpL22-like ribosomes in S2 cells. (A) Western blot analysis of wild-type testis and sperm. Shal protein is found in mature sperm but not in whole testis. eRpL22-like is found in the whole testis. (B) RT-PCR analysis of wild-type (WT) and *cannonball*^{12} meiotic mutant (*can*^{12}) testis. *shal* is detected at the expected molecular weight (85 base pairs) in both WT and *can*^{12} testis suggesting some *shal* mRNA is transcribed before the G2/M transition in meiosis I. Agarose gel 1.5%. NTC is no template control. Gel is cropped to show the lower third of the gel. The PCR band seen at below 75 base pairs (see arrowhead) is indicative of primer dimers in all agarose gels shown. (C) Western blot analysis of TIMP shows a weak signal in whole testis. eRpL22-like is also found in the testis. (D) RT-PCR analysis of WT and *can*^{12} testis. *timp* can be detected at the expected molecular weight (87 base pairs) in both WT and *can*^{12} testis confirming *timp* mRNA is primarily transcribed early in spermatogenesis. Agarose gel 1.5%. NTC is no template control. Gel is cropped to show the lower third of the gel. (E) IHC of wild-type testis stained with eRpL22-like (green) and TIMP (red) shows TIMP, along with eRpL22-like, is expressed in spermatocytes. Magnification 20×. Apical tip is denoted with an asterisk. (F) Shal protein can be translated in both S2 cells (expresses eRpL22 but not eRpL22-like) and FLAG–eRpL22-like S2 cells (expresses eRpL22 and eRpL22-like). This suggests Shal can be translated on either eRpL22- or eRpL22-like ribosomes in S2 cells, which differs from its association in the testis. Shal is expressed from a pMT plasmid with 500 μM $CuSO_4$. eRpL22-like can only be found in FLAG–eRpL22-like S2 cells. (G) TIMP protein can be translated in both S2 and FLAG–eRpL22-like S2 cells suggesting TIMP can be translated on either eRpL22 paralogue-specific ribosome type. TIMP is expressed from a pMT plasmid with 500 μM $CuSO_4$. FL: FLAG–eRpL22-like S2 cells.

eRpL22-like ribosomes within FLAG–eRpL22-like S2 cells.

Within FLAG–eRpL22-like S2 cells, more *timp* mRNA was found in association with eRpL22-like protein (fold change: 3.05; SD: ±2.3), suggesting that preferential loading onto eRpL22-like ribosomes (as shown in the testis) can be replicated within this S2 cell line. As was the case with *shal* mRNA, less *timp* mRNA was also loaded onto eRpL22 ribosomes in FLAG–eRpL22-like S2 cells (fold change: 0.52; SD: ±0.5). The apparent preferential loading and translation of both *shal* and *timp* mRNAs on eRpL22-like ribosomes within FLAG–eRpL22-like S2 cells notably occurs in the absence of testis-specific factors (summarized in Table 3). These results also demonstrate that *shal* and *timp* mRNAs are not excluded from association with eRpL22 ribosomes within S2 cells. Whether or not a specific mechanism exists to exclude specific mRNAs from associating with specific ribosomes in the testis remains unknown. It is possible that the apparent loading preference of these mRNAs onto eRpL22-like ribosomes within both FLAG–eRpL22-like S2 cells and also within post-meiotic spermatocytes in the testis is a default outcome based on abundance of eRpL22-like ribosomes relative to eRpL22 ribosomes within the cytoplasm in both instances.

Importantly, preferential association of *shal* and *timp* mRNAs with eRpL22-like ribosomes within our S2 cell model simulates results for these mRNAs from our testis RNA-seq experiments, and suggests that testis-specific factors are not essential to drive association of these mRNAs with eRpL22-like ribosomes.

DISCUSSION

Specialized translation in specific stages of spermatogenesis and its implications

In this study, heterogeneous populations of ribosomes, distinguished by eRpL22 paralogue content, were isolated from the adult *Drosophila* testis using paralogue-specific IPs from polysome profiles. Precipitated polysomes contain one paralogue type (either eRpL22 or eRpL22-like depending on antibodies used), but not a mixture of both types within the same IP; that is, polysomes appear to be homogeneous with regard to eRpL22 or eRpL22-like. Other polysome composition differences (not assessed in these studies) may exist and contribute to variability between eRpL22 paralogue-specific polysome replicates.

Gene name	Protein expression	RNA expression	RNA sequencing	S2 cell expression	qRT-PCR	eRpL22 ribosome association in S2 cells
shal	Mature sperm, not in whole testis	Before G2/M transition of meiosis I	Fold change: 8.2 eRpL22-like ribosomes	S2 and FLAG–eRpL22-like S2 cells	Fold change: 4.8 FLAG–eRpL22-like ribosomes	Fold change: 0.13 Less *shal* on eRpL22 ribosomes in FLAG–eRpL22-like S2 cells
timp	Testis	Before G2/M transition of meiosis I	Fold change: 6.9 eRpL22-like ribosomes	S2 and FLAG–eRpL22-like S2 cells	Fold change: 3.05 FLAG–eRpL22-like ribosomes	Fold change: 0.52 Less *timp* on eRpL22 ribosomes in FLAG–eRpL22-like S2 cells

TABLE 3: Summary of Shal and TIMP specialized ribosome data.

Mechanisms controlling polysome homogeneity with respect to eRpL22 paralogue content remain unclear, but specificity is likely to be determined at the level of initiation complex formation. It is unknown how eRpL22 paralogue homogeneity within polysomes impacts translation regulation or may control translation rates for specific mRNAs.

Characterization of mRNAs from testis polysomes by RNA sequencing revealed more than 12,000 transcripts found in association with eRpL22 paralogue-specific ribosomes. From the collection of mRNAs obtained from paralogue-specific polysome IPs, unique and overlapping translatomes were uncovered for each ribosome type. This investigation is the first report of specialized ribosomes based on Rp paralogue content in *D. melanogaster*.

Spermatogenesis in *Drosophila* is a complex process requiring numerous testis-specific transcripts for sperm maturation (Chintapalli *et al*., 2007). The translatomes for eRpL22 paralogue-specific polysomes differ significantly in the testis. Many transcripts required during early mitotic and meiotic phases are found on both polysome types or are associated primarily with eRpL22 ribosomes. As sperm maturation continues past meiosis I, a significant switch in eRpL22 localization from cytoplasm to the nucleus and nucleoplasm occurs within primary spermatocytes, likely regulated by germ cell–specific eRpL22 SUMOylation and phosphorylation (Kearse *et al*., 2013). Subcellular redistribution of eRpL22 may remove a large pool of eRpL22 ribosomes from the active translation pathway, leaving the majority as eRpL22-like ribosomes. Interestingly, the majority of transcripts known to be required postmitotically during meiosis and in spermiogenesis associate with eRpL22-like polysomes. Transcripts expressed postmitotically may be loaded onto eRpL22-like ribosomes by default due to their abundance in the ribosomal pool (see model; Figure 5). Alternatively, a preferential loading mechanism may be required for eRpL22-like ribosome association.

cup and *comet* genes are transcribed after meiosis, but transcripts are stored as translationally inactive complexes (by unknown mechanisms) until later stages of spermiogenesis (Barreau *et al*., 2008). The presence of *Marf* (among others) and a small group of *cup* transcripts on eRpL22 ribosomes confirms that at least a small pool of eRpL22 ribosomes persists into spermiogenesis stages well after nucleoplasmic sequestration of the majority of eRpL22 in postmeiotic, elongating spermatocytes. The majority of transcripts in this postmeiotic group associates with either polysome type. *Ryder-cup* transcripts are preferentially loaded onto eRpL22-like polysomes. Additionally, loading of *cup* transcripts onto eRpL22 ribosomes, while in the presence of an abundance of eRpL22-like ribosomes, suggests a mechanism to specifically target these transcripts to eRpL22 ribosomes or alternatively, a mechanism that excludes these *cup* transcripts from eRpL22-like ribosomes. It is reasonable to propose that a specific mechanism exists to target some transcripts (e.g., *stanley-cup*) to eRpL22 ribosomes (notwithstanding the high concentration of eRpL22-like ribosomes).

While the translatome of eRpL22-like polysomes includes predominantly testis-specific mRNAs, meiotic- and later-stage transcripts, other mRNA types were captured that have not previously been studied in the testis. *shal* and *timp* transcripts have been studied extensively in the nervous system. Their presence on testis-specific ribosomes presents intriguing possibilities that may connect gene functions to critical events in sperm development or postfertilization events important in early embryogenesis.

Previous work by Shi *et al*. (2017) revealed that eRpL22 stoichiometry in mouse embryonic stem cell (mESC) polysomes does not differ significantly compared with levels in free 60S subunits. In other cases, levels of specific Rps were diminished relative to amounts in free subunits, indicating that in some cases, polysomes were devoid of a core Rp. The eRpL22 result in mESCs suggests that this Rp may not contribute extensively to ribosome heterogeneity in defining populations of specialized ribosomes in this cell type.

In *Drosophila,* however, both paralogues are essential (eRpL22: Bourbon *et al*., 2002; Boutros *et al*., 2004; eRpL22-like: Mageeney *et al*., 2018), indicating that eRpL22 paralogues in *Drosophila* may have selective roles in translation that differ from their roles in other organisms (such as mice and humans) where depletion or removal from ribosomes is not lethal (Anderson *et al*., 2007; Houmani and Ruf, 2009). Our work highlights the fact that eRpL22- or eRpL22-like ribosomes within the *Drosophila* male germline are specialized and functionally distinguishable by association with different RNA subpopulations. eRpL22 may therefore function differently as a component of specialized ribosomes controlling specific mRNA translation, depending on the organism in question, the developmental stage, or the state of tissue differentiation.

From large-scale genetic screens in *Drosophila*, it is clear that not all genes enriched in males or expressed in the testis are required for fertility (e.g., Wakimoto *et al*., 2004). Global deficiencies in specialized translation of transcripts affecting fertility are among the factors that could contribute to a spectrum of phenotypes leading to male infertility. Our previous studies showed that eRpL22 and eRpL22-like are partially functionally redundant, yet specify unique roles in spermatogenesis as well. Fertility defects in flies depleted in eRpL22 and partially rescued with eRpL22-like overexpression (Mageeney *et al*., 2018) may be attributable to insufficient translation of key proteins. Overall, this study provides a new model for focusing on the potential impact of ribosome heterogeneity and specialized translation in effecting fertility.

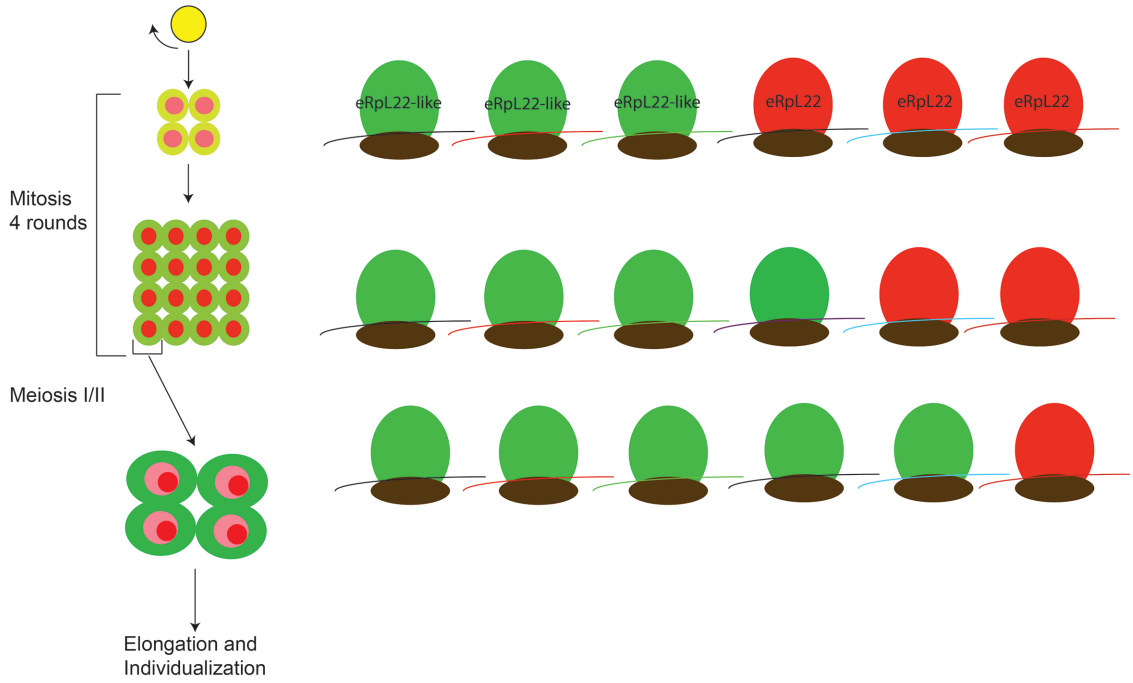

FIGURE 5: Model for eRpL22 paralogue-specific ribosomes. Early in spermatogenesis both eRpL22 paralogues (eRpL22 [red] and eRpL22-like [green]) are coexpressed in the cytoplasm and are components of the ribosome. Data support this proposal in two ways: (1) most testis transcripts are transcribed early in spermatogenesis and (2) a large population of RNAs with no preference for either eRpL22 paralogue-specific ribosome was recovered in the RNA-sequencing data set. As spermatogenesis progresses into meiotic and later stages, eRpL22 localizes to the nucleoplasm, with a smaller population remaining in the cytoplasm. eRpL22-like is cytoplasmic at all stages of spermatogenesis. In these later stages it is presumed eRpL22-like is the primary ribosomal component and is translating the bulk of testis-specific RNAs. eRpL22 is still a component of the ribosome in these stages but there are fewer eRpL22 ribosomes than eRpL22-like ribosomes. The impact of other Rp paralogous, ncRNAs, or testis-specific RAPs on eRpL22 paralogue-specific ribosomes is currently unknown, but may contribute to specific mRNA loading.

Mechanistic insights for loading mRNAs onto paralogue-specific specialized ribosomes

With mounting evidence for the existence of specialized ribosomes in several systems (recently reviewed by Genuth and Barna, 2018; Gerst, 2018), major questions have emerged about mechanisms that direct specialized translation on a subset of heterogeneous ribosomes. Within the *Drosophila* male germline, specific mRNA recognition is expected to include distinguishing features of the paralogues themselves and *cis*-acting structural features within the mRNAs.

Notable structural differences between *Drosophila* eRpL22 paralogues and other eRpL22 orthologues are apparent (Kearse *et al.*, 2011), with fly N- and C-terminal extensions projecting from the subunit surface, available for interactions on the solvent side (Anger *et al.*, 2013). Although eRpL22/eRpL22-like is positioned away from the subunit interface where interaction with a 43S preinitiation complex would take place, it is possible that mRNA–paralogue-specific ribosome interactions are facilitated by ribosome binding proteins that create an interface between eRpL22 or eRpL22-like within the 60S subunit and a specific mRNA within the preinitiation complex. It is noteworthy that Simsek *et al.* (2017) identified ribosome-associated proteins (RAPs) that increase ribosome heterogeneity and allow for specific loading of mRNA onto ribosomal subpopulations. Potential interactions between RAPs and eRpL22 paralogue-specific ribosomes may further contribute to translatome specificity.

If RAPs of this sort function at specific stages of spermatogenesis, it is unclear whether these proteins are ubiquitously expressed in many cell types and tissues or whether these proteins are germline-specific. Ectopic expression of *shal* and *timp* mRNA in S2 cells addressed the question of whether loading of mRNA onto eRpL22-like ribosomes requires cell-specific RAPs. Both mRNAs were preferentially loaded onto eRpL22-like ribosomes in transfected S2 cells, mimicking the testis pattern. A greater concentration of eRpL22-like ribosomes in FLAG–eRpL22-like S2 cells and in meiotic and post-meiotic germ cells may favor association of these mRNAs with this ribosome subpopulation, without invoking a specific targeting mechanism. We cannot as yet exclude this possibility. We can, however, conclude that no germline-specific factors (that may include testis-specific RAPs) are necessary for *shal* and *timp* mRNA loading onto eRpL22-like ribosomes within S2 cells. If RAPs are required, then these factors must be present in both germline and S2 cells. Expression of *shal* and *timp* mRNAs in control S2 cells suggests that no mechanism exists in S2 cells to exclude these RNAs from translation on eRpL22 ribosomes. Whether or not this is also the case within the germline is unknown.

RNA features relevant for selective mRNA recognition by eRpL22 paralogue-specific ribosomes are unknown. A conserved mRNA sequence or conserved element was identified for mRNA recognition by eRpL38-specific ribosomes in mESCs (Xue *et al.*, 2015). Computational analyses using Clustal Omega (Goujon *et al.*, 2010; Sievers *et al.*, 2011; McWilliam *et al.*, 2013) and mFOLD analyses (Zuker, 2003) did not identify conserved sequence motifs or conserved secondary structural features within untranslated or coding regions of the top 40 transcripts for each ribosome type or within subgroups of

mRNAs identified from specific stages of spermatogenesis. Analysis of the entire RNA-seq data set will be required for a comprehensive understanding of conserved mRNA features.

ncRNAs found in association with specialized eRpL22 paralogue-specific polysomes may play regulatory roles

ncRNAs display an extensive capacity for regulating gene expression and show complex patterns of subcellular nuclear and cytoplasmic accumulation (reviewed by Cech and Steitz, 2014). Most ncRNAs identified in our study have not been studied extensively. Recent studies suggest that lncRNAs are crucial for *Drosophila* spermatogenesis (Wen *et al*., 2016). Knockout of these ncRNAs using CRISPR methods caused defects in late stages of spermatogenesis. Several of the lncRNAs identified in the Wen *et al*. (2016) study are found in association with paralogue-specific polysomes identified in this study. It is plausible that some of these molecules function as translation regulators. Many testis transcripts are transcribed and translated early in spermatogenesis as part of the maturation process from mitosis into meiotic stages. Several mRNAs are translationally repressed by unknown mechanisms until later stages of spermatogenesis (reviewed by Schäfer *et al*., 1995). We speculate that some ncRNAs may play a role in translation repression, even though isolated in a polysome context, typically presumed to be translationally active. ncRNAs might also play a role in translation derepression, thereby specifying when and possibly on what ribosome type, translation would occur.

Numerous snoRNAs associate with eRpL22 paralogue-specific polysomes, with a larger proportion associating with eRpL22-like polysomes. Recent reports show that snoRNAs can be further processed into snoRNA-derived small RNAs (called sd-RNAs) with noncanonical roles (reviewed by Scott and Ono, 2011). Furthermore, snoRNAs and sd-RNAs have been implicated in pathways apart from rRNA modifications in ribosomes (reviewed by Scott and Ono, 2011). The majority of box C/D snoRNAs are enriched in the nucleus, but a small proportion is cytoplasmic. In some cases snoRNAs function like miRNAs (Ender *et al*., 2008).

We recently uncovered a novel mechanism of cross-talk between eRpL22 paralogues, suggesting a negative regulatory effect of eRpL22-like on eRpL22 mRNA and protein levels in the testis (Mageeney *et al*., 2018). The mechanism controlling this process is no doubt complex, likely involving different levels of regulation including translation. *erpL22* mRNA is translated on both polysome types, with a slight preference for translation on eRpL22 ribosomes. Three of four ncRNAs transcribed from the *erpL22* genomic locus are found in association with eRpL22-like polysomes and may target specific mRNAs (including *erpL22*) on that population of ribosomes or alternatively, be sequestered on these ribosomes away from their primary site of action. Associated ncRNAs may affect *erpL22* mRNA stability or translation on eRpL22-like polysomes, providing a link to cross-talk regulation uncovered in RNAi-mediated depletion studies in the testis (Mageeney *et al*., 2018).

MATERIALS AND METHODS

Fly stocks

Oregon R wild-type flies were used in this study. *cannonball* (*can*) (w; can[12]/TM3, Sb) meiotic mutant flies were a kind gift from Margaret (Minx) Fuller of Stanford University (Lin *et al*., 1996).

Tissue collection

Testis (2- to 10-d-old adults) were dissected in sterile 1X phosphate-buffered saline (PBS) and frozen immediately on dry ice. Testis samples were used immediately or stored at –80°C until used for further analysis.

Antibodies

Rabbit polyclonal anti-eRpL22 and mouse polyclonal anti-eRpL22–like antibodies (developed by Kearse *et al*. 2011) were used at 1:1000 for Western blot analysis and 1:100 for IHC. eRpL22 antibody used for Western blot analysis was lot 7815 and lot 7817 for IHC. These are different from lots used in Kearse *et al*. (2011, 2013). Anti-rabbit polyclonal eRpL9 (Santa Cruz; #AP16409b) was used at 1:300 for Western blot analysis. Rabbit polyclonal anti-eRpL23a (Abgent; #AP1939b) was used at 1:1000 for Western blot analysis. Chicken anti-*Drosophila* peptide polyclonal anti-eRpL23a antibody (produced by Genscript, using the following peptide sequence from FlyBase [Crosby *et al*., 2007]: CRDYDALDIANKIGII, and specificity confirmed by comparison with rabbit polyclonal anti-eRpL23a in Western blots) was used at 1:13,000 for Western blot analysis. Rabbit polyclonal anti-Shal (a kind gift from Susan Tsunoda at Colorado State University; Diao *et al*., 2009) was used at 1:50 for Western blot analysis. Rabbit polyclonal anti-TIMP (a kind gift from Kendal Broadie at Vanderbilt University; Dear *et al*., 2016) was used at 1:2000 for Western blot analysis and 1:500 for IHC. Secondary HRP-conjugated goat anti-mouse IgG (#W4021) and goat anti-rabbit IgG (#Q4011) antibodies were obtained from Promega and used at 1:50,000 for Western blot analysis. Goat–anti-mouse/Alexa Fluor 488 and goat–anti-rabbit/Alexa Fluor 568 were obtained from Invitrogen (#A11029 and #A11036, respectively) were used at 1:200 for IHC.

Immunohistochemistry

Testis squashes and immunostaining were performed as previously described (Kearse *et al*., 2011). Briefly, testis tissue was squashed with a #1 coverslip onto a glass slide and immediately frozen on dry ice. Tissue was fixed in ice-cold ethanol and 4% formaldehyde and washed two times in PBST with sodium deoxycholate (1X PBS, 0.3% sodium deoxycholate, 0.3% Triton X-100) and one time in PBST. Tissue was then incubated overnight in primary antibody, washed four times in PBTB (1X PBS, 0.1% bovine serum albumin [BSA], 0.1% Triton X-100), and incubated for 1 h in secondary antibody. Tissue was washed four times in PBTB, followed by two times in 1X PBS and mounted using Fluormount-G (Southern Biotech; #0100-01). Imaging was completed using a Nikon Eclipse TE200U.

Polysome profile analysis

Ribosome extracts were prepared using modified procedures described in Kearse *et al*. (2011). Adult testes pairs from 8000 males were dissected in PBS (without cycloheximide added) in batches, transferred to microcentrifuge tubes on dry ice, and subsequently stored frozen at –80°C until all tissue was collected. Frozen testes were then homogenized in lysis buffer (20 mM Tris-HCl, pH 7.4, 140 mM KCl, 5 mM $MgCl_2$, 0.5 mM dithiothreitol [DTT], 1% Triton X-100) with 100 µg/ml cycloheximide (1:5 wt/vol; Qin *et al*., 2007) and incubated on ice for 10 min. Homogenates were then cleared by centrifugation for 10 min at 17,000 × *g*. One-fourth of the sample was loaded onto a 10–50% linear sucrose gradient (prepared by methods described in Houmani and Ruf, 2009) for four different gradients and spun at 209,490 × *g* for 160 min in a SW-41 rotor (Beckman Coulter) at 4°C. Gradient fractions (0.5 ml) were collected and OD600 was read by a Teledyne Isco UA-6 detector.

Immunoprecipitation

Immunoprecipitation was performed as described in Inada *et al*. (2002) with modifications. One hundred fifty microliters of the 0.5 ml fraction corresponding to polysomes (determined by spectrophotometry peaks) were incubated with either 26.25 µg eRpL22 or

eRpL22-like antibody overnight rotating at 4°C. PureProteome Protein A/G mix magnetic bead (Millipore; #LSKMAGA02) were added to each sample and incubated for 3 h rotating at 4°C. Beads were washed three times with 1X IA-100 buffer (50 mM Tris-HCl, pH 7.5, 100 mM KCl, 2 mM $Mg(OAc)_2$, 1 mM DTT, 1 mM phenylmethylsulfonyl fluoride). Ribosomes were eluted from beads using 100 µg/ml corresponding paralogue-specific peptide (created by Genscript; described in Kearse *et al.*, 2011).

RNA isolation from IP

RNA was isolated from IP eluates as described in Inada *et al*. (2002) with some modifications. Paralogue-specific IP eluates were incubated with 0.1 mg/ml proteinase K in proteinase K buffer (0.2 M Tris-HCl, pH 7.5, 0.3 M NaCl, 2% SDS, 25 mM EDTA) for 45 min at 37°C. RNA was extracted twice with a 1:1 phenol:chloroform mix, then one time with chloroform and stored overnight in 100% isopropanol. Samples were washed with 70% ethanol and resuspended in diethyl pyrocarbonate (DEPC)-treated water.

RNA isolation from tissue

Testis tissue and cDNA synthesis was performed as previously described (Kearse *et al.*, 2011).

RNA sequencing

RNA sequencing was performed by the Duke Center for Genomic and Computations Biology. RNA-sequencing data can be accessed at Gene Expression Omnibus (GEO) under accession number GSE124371. Four RNA replicates per paralogue-specific ribosome population were amplified using the Clonetech low input SMARTer mRNA amplification kit. A cDNA library was created using the Kapa Hyper prep kit. The cDNA quality was analyzed by the Agilent 2100 bioanalyzer (High Sensitivity DNA application) and the libraries were sequenced on an Illumina Hi-seq 4000 (50 base pairs SR).

Analysis of RNA-sequencing results

RNA analysis was done at Duke University Genomic Analysis and Bioinformatics Shared Resource Core. Sequencing reads were processed with the TrimGalore toolkit (http://www.bioinformatics.babraham.ac.uk/projects/trim_galore), which cut low quality bases and Illumina sequencing adapters from the 3′ end of the reads using the tool Cutadapt (Martin, 2011). Sequencing reads that were longer than 20 nt were kept for further analysis and mapped using the STAR RNA-seq alignment tool (Dobin *et al*., 2012) to the r6v15 version of the *Drosophila melanogaster* genome and transcriptome (Gramates *et al*., 2017). Reads that mapped to a single genomic locus and had at least 10 reads per gene (compiled by HTSeq tool [http://www-huber.embl.de/users/anders/HTSeq/]) were used in subsequent analysis. The DESeq2 (Love *et al*., 2014) Bioconductor (Huber *et al*., 2015) package with the R statistical programming environment (www.r-project.org) was used for normalization and differential expression analysis and the false discovery rate was calculated for multiple hypothesis tests. Pathways enriched for differentially expressed genes with a p value ≤ 0.05 and a log2(FC) > 1 or < −1 were analyzed using the DAVID pathway analysis suite (Huang *et al*., 2009). Bioinformatics for single genes was carried out for ~2000 transcripts by searching for the gene in FlyBase (Gramates *et al*., 2017). Data pertaining to molecular function, biological process, transcript, and polypeptide expression were characterized for each gene product. The Gene Ontology Consortium was used to determine enrichment for different biological processes, by inputting FlyBase geneIDs for each gene found in the different ribosome populations (Ashburner *et al*., 2000; GO Consortium, 2017; Mi *et al*., 2017).

Data discussed in this study have been deposited in NCBI's Gene Expression Omnibus (Edgar *et al*., 2002; Barrett *et al*., 2013) and are accessible through GEO Series accession number GSE124371 (https://www.ncbi.nlm.nih.gov/geo/query/acc.cgi?acc=GSE124371).

Western blot analysis

SDS–PAGE analysis was used to separate proteins that were then electroblotted onto Westran-S PVDF membrane (Whatman; 310413096) for 1 h in chilled transfer buffer. Membranes were blocked in 5% nonfat dry milk (NFDM) for 1 h at 4°C and incubated with primary antibody in 3% NFDM overnight at 4°C. Membranes were washed in wash buffer and HRP-conjugated secondary antibodies were incubated at 4°C for 2 h. ECL2 (Thermo Scientific; #PI80196) was used for chemiluminescence detection with Kodak Bio-Max film (Kodak).

RT-PCR

RNA from RNA-sequencing samples was used for RT-PCR experiments. cDNA was created using the Invitrogen first-strand superscript synthesis kit following the manufacturer's guidelines as described in Kearse *et al*. (2011). PCR was performed as follows: 10 µM forward and reverse primer (primers in Supplemental Table 2), 1 µl cDNA, platinum blue PCR supermix (Invitrogen; #12580-015). PCR cycling conditions were 95°C for 5 min, 35 cycles: 95°C for 1 min, Tm-5°C for 30 s, 72°C for 1 min/kb, followed by final elongation at 72°C for 10 min. PCR products were run on a 2% agarose gel in Tris acetate EDTA (TAE) buffer.

Cloning

The FLAG–eRpL22-like construct for expression in a S2 stable line was created by standard PCR methods from previously isolated cDNA (Kearse *et al*., 2011). A FLAG tag was incorporated by adding the FLAG coding sequence into the forward primer (primers in Supplemental Table 2) and cloned into pMT/V5-His-TOPO (Invitrogen; #K412501) following the manufacturer's recommendations. pCoBlast plasmid was used as a selection plasmid for stable lines and was obtained from Invitrogen (#K512001). cDNA plasmids for timp (#2288) and shal (#9239) were obtained from the *Drosophila* Genomic Resource Center and subcloned by standard PCR methods with Platinum Taq DNA Polymerase High Fidelity (Invitrogen; #11304011). Primers included both the 5′ and 3′ UTR sequences and a *Spe*I restriction site to allow for cloning into pMT/V5-His version A (primers listed in Supplemental Table 2). All plasmids were sequenced for accuracy.

Cell culture

S2 cells were obtained from *Drosophila* Genomics Resource Center (Stock #6) and cultured at 26°C in Schneider's *Drosophila* media (Invitrogen; #21720024) supplemented with 10% heat-inactivated fetal bovine serum (Invitrogen; #10082). To create the S2/pMT_FLAG–eRpL22-like stable line, cells were seeded at 1×10^6 cell ml^{-1}. Transfections using 19 µg of pMT/FLAG–eRpL22-like and 1 µg of pCo/Blast were completed 16 h later, following the guidelines in the Invitrogen calcium phosphate transfection kit (Invitrogen; #K278001). Twenty-four hours later the transfection was washed out with fresh media. The cells were incubated at 28°C for 48 h and 25 µg ml^{-1} BlasticidinS (Invitrogen; #R21001) was used as a selection agent. Cells were expanded out and kept under BlasticidinS selection.

Cell culture transfections

Wild-type S2 cells or S2/pMT_FLAG–eRpL22-like cells were seeded 1×10^6 (6 ml/t-flask) and induced with a final concentration of

500 μM $CuSO_4$ and incubated for 28 h. Cells were then washed two times in fresh media and seeded 1×10^6 (3 ml/well) and incubated 16 h. Cells were transiently transfected with either 19 μg of pMT/*shal* or pMT/*timp* DNA using the calcium phosphate transfection kit (Invitrogen; #K278001). Cells were washed 24 h posttransfection and induced 8 h later with 500 μM $CuSO_4$ final. Samples were taken 5 d posttransfection. See schematic Supplemental Figure 4.

qRT-PCR

RNA was isolated as described above from IP samples. cDNA and qPCR specification were previously described in Kearse *et al*. (2011). Expression levels were normalized to *eRpL32* (ΔCT). Fold change between eRpL22 and eRpL22-like ribosomal population in FLAG–eRpL22-like S2 cells was determined by first calculating ΔΔCT = ΔCT (FLAG–eRpL22-like S2 cells/eRpL22-like IP) – ΔCT (FLAG–eRpL22-like S2 cells/eRpL22 IP), and then calculating fold change as $2^{-\Delta\Delta CT}$. Fold change for eRpL22 polysomes was determined by first calculating ΔΔCT = ΔCT (FLAG–eRpL22-like S2 cells/eRpL22 IP) – ΔCT (S2 cells/eRpL22 IP), and then calculating fold change as $2^{-\Delta\Delta CT}$. Primers used can be found in Supplemental Table 2.

ACKNOWLEDGMENTS

Financial support was provided in part by Lehigh University faculty research funds and National Institutes of Health 1R15GM-132889-01 to V.C.W. The work described here is in partial fulfillment of the requirements for the PhD degree for C.M.M., who was partially funded by a Nemes Fellowship from Lehigh University. We thank members of the fly community (noted in *Materials and Methods*) for sharing of reagents, David Corcoran from Duke Bioinformatics Core for assistance with RNA-seq data analysis, Julie Haas from Lehigh University for Matlab assistance, and Lee Graham from Lehigh University for core equipment maintenance. Members of C.M.M.'s dissertation committee are acknowledged for thoughtful discussion and feedback about this work and the manuscript.

REFERENCES

Anderson SJ, Lauritsen JP, Hartman MG, Foushee AM, Lefebvre JM, Shinton SA, Gerhardt B, Hardy RR, Oravecz T, Wiest DL (2007). Ablation of ribosomal protein L22 selectively impairs αβ T cell development by activation of a p53-dependent checkpoint. Immunity 26, 759–772.

Anger AM, Armache JP, Berninghausen O, Habeck M, Subklewe M, Wilson DN, Beckmann R (2013). Structures of the human and *Drosophila* 80S ribosome. Nature 497, 80–85.

Ashburner M, Ball CA, Blake JA, Botstein D, Butler H, Cherry JM, Davis AP, Doliski K, Dwight SS, Eppig JT, *et al*. (2000). Gene ontology: tool for the unification of biology. The Gene Ontology Consortium. Nat Genet 25, 25–29.

Baker CC, Gum BS, Fuller MT (2015). Cell type-specific translational repression of Cyclin B during meiosis in males. Development 142, 3394–3402.

Barreau C, Benson E, Gudmannsdottir E, Newton F, White-Cooper H (2008). Post-meiotic transcription in *Drosophila* testes. Development 135, 1897–1902.

Barrett T, Wilhite SE, Ledoux P, Evangelista C, Kim IF, Tomashevsky M, Marshall KA, Phillippy KH, Sherman PM, Holko M, *et al*. (2013). NCBI GEO: archive for functional genomics data sets—update. Nucleic Acids Res 41, D991–D995.

Ben-Shem A, Garreau de Loubresse N, Melnikov S, Jenner L, Yusupova G, Yusupov M (2011). The structure of the eukaryotic ribosome at 3.0 Å resolution. Science 334, 1524–1529.

Bourbon HM, Gonzy-Treboul G, Peronnet F, Alin MF, Ardourel C, Benassayag C, Cribbs D, Deutsch J, Ferrer P, Haenlin M, *et al*. (2002). A P-insertion screen identifying novel X-linked essential genes in *Drosophila*. Mech Dev 110, 71–83.

Boutros M, Kiges AA, Armknecht S, Kerr K, Hild M, Koch B, Haas SA, Paro R, Perrimon N, Heidelberg Fly Array Consortium (2004). Genome-wide RNAi analysis of growth and viability in *Drosophila* cells. Science 303, 832–835.

Cech TR, Steitz JA (2014). The noncoding RNA revolution—trashing old rules to forge new ones. Cell 157, 77–94.

Chintapalli V, Wang J, Dow J (2007). Using FlyAtlas to identify better *Drosophila* models of human disease. Nat Genet 39, 715–720.

Crosby MA, Goodman JL, Strelets VB, Zhang P, Gelbart WM, FlyBase Consortium (2007). Flybase: genomes by the dozen. Nucleic Acids Res 35, 486–491.

Dear ML, Dani N, Parkinson W, Zhou S, Broadie K (2016). Two classes of matrix metalloproteinases reciprocally regulate synaptogenesis. Development 143, 75–87.

Diao F, Waro G, Tsunoda S (2009). Fast inactivation of Shal (K(v)4) K+ channels is regulated by the novel interactor SKIP3 in *Drosophila* neurons. Mol Cell Neurosci 42, 33–44.

Dobin A, Davis CA, Schlesinger F, Drenkow J, Zaleski C, Jha S, Batut P, Chaisson M, Gingeras TR (2012). STAR: ultrafast universal RNA-seq aligner. Bioinformatics 29, 15–21.

Dorus S, Busby SA, Gerike U, Shabanowitz J, Hunt DF, Karr TL (2006). Genomic and functional evolution of the *Drosophilamelanogaster* sperm proteome. Nat Genet 38, 1440–1445.

Edgar R, Domrachev M, Lash AE (2002). Gene Expression Omnibus: NCBI gene expression and hybridization array data repository. Nucleic Acids Res. 30, 207–210.

Ender C, Krek A, Friedlander MR, Beitzinger M, Weinmann L, Chen W, Pfeffer S, Rajewsky N, Meister G (2008). A human snoRNA with microRNA-like functions. Mol Cell 32, 519–528.

Fisher BE, Wasbrough E, Meadows LA, Randlet O, Dorus S, Karr TL, Russell S (2012). Conserved properties of *Drosophila* and human spermatozoal mRNA repertoires. Proc R Soc Lond B Biol Sci 279, 2636–2644.

Fuller MT (1993). Spermatogenesis. In: The Development of *Drosophila*, ed. M Bate, Cold Spring Harbor, NY: Cold Spring Harbor Press. 171–147.

Fuller MT (2016). Differentiation in stem cell lineages and in life: explorations in the male germ line stem cell lineage. Curr Top Dev Biol 116, 375–390.

The Gene Ontology Consortium (2017). Expansion of the gene ontology knowledgebase and resources. Nucleic Acids Res 45, D331–D338.

Genuth NR and Barna M (2018). The discovery of ribosome heterogeneity and its implications for gene regulation and organismal life. Mol Cell 71, 364–374.

Gerst JE (2018). Pimp my ribosome: ribosomal protein paralogs specify translational control. Trends Genet 34, 832–845.

Ghosh S, Lasko P (2015). Loss-of-function analysis reveals distinct requirements of the translation initiation factors eIF4E, eIF4E-3, eIF4G and eIF4G2 in *Drosophila* spermatogenesis. PLoS One. 10, e01225.

Goujon M, McWilliam H, Li W, Valentin F, Squizzato S, Paern J, Lopez R (2010). A new bioinformatics analysis tools framework at EMBL-EBI. Nucleic Acids Res 38, W695–W699.

Gramates LS, Marygold SJ, dos Santos G, Urbano J-M, Antonazzo G, Matthews BB, Rey AJ, Tabone CJ, Crosby MA, Emmert DB, *et al*. and the FlyBase Consortium (2017). FlyBase at 25: looking to the future. Nucleic Acids Res 45, D663–D671.

Houmani JL, Ruf IK (2009). Clusters of basic amino acids contribute to RNA binding and nucleolar localization of ribosomal protein L22. PLoS One 4, e5306.

Hempel LU, Rathke C, Raja SJ, Renkawitz-Pohl R (2006). In *Drosophila*, *don juan* and *don juanlike* encode proteins of the spermatid nucleus and the flagellum and both are regulated at the transcriptional level by the TAFII80 cannonball while translational repression is achieved by distinct elements. Dev Dyn 235,1053–1064.

Huang da W, Sherman BT, Lempicki RA (2009). Bioinformatics enrichment tools: paths toward the comprehensive functional analysis of large gene lists. Nucleic Acids Res 37, 1–13.

Huber W, Carey VJ, Gentleman R, Anders S, Carlson M, Carvalho BS, Bravo HC, Davis S, Gatto L, Girke T, *et al*. (2015). Orchestrating high-throughput genomic analysis with Bioconductor. Nat Methods 12, 115–121.

Inada T, Winstall E, Tarun SZ, Yates JR, Schieltz D, Sachs AB (2002). One-step affinity purification of the yeast ribosome and its associated proteins and mRNAs. RNA 8, 948–958.

Kai T, Williams D, Spradling AC (2005). The expression profile of purified *Drosophila* germline stem cells. Dev Biol 283, 486–502.

Kearse MG, Chen AS, Ware VC (2011). Expression of ribosomal protein L22e family member in *D. melanogaster*: rpL22-like is differentially expressed and alternatively spliced. Nucleic Acids Res 39, 2701–2716.

Kearse MG, Ireland JA, Prem SM, Chen AS, Ware VC (2013). RpL22e, but not RpL22e-like-PA, is SUMOylated and localizes to the nucleoplasm of *Drosophila* meiotic spermatocytes. Nucleus 4, 241–258.

Komili S, Farny NG, Roth FP, Silver PA (2007). Functional specificity among ribosomal proteins regulates gene expression. Cell 131, 557–571.
Kondrashov N, Pusic A, Stumof CR, Shimizu K, Hsieh AC, Xue S, Ishijima J, Shiroishi T, Barna M (2011). Ribosome-mediated specificity in Hox mRNA translation and vertebrate tissue patterning. Cell 14, 383–397.
Koyama Y, Katagiri S, Hanai S, Uchida K, Miwa M (1999). Poly(ADP-ribose) polymerase interacts with novel *Drosophila* ribosomal proteins, L22 and L23a, with unique histone-like amino-terminal extensions. Gene 226, 339–345.
Li MA, Alls JC, Avancini RM, Koo K, Godt D (2003). The large Maf factor Traffic jam controls gonad morphogenesis in *Drosophila*. Nat Cell Biol 5, 994–1000.
Lim C, Tarayrah L, Chen X (2012). Transcriptional regulation during *Drosophila* spermatogenesis. Spermatogenesis 2, 158–166.
Lin TY, Viswanathan S, Wood C, Wilson PG, Wolf N, Fuller MT (1996). Coordinated developmental control of the meiotic cell cycle and spermatid differentiation in *Drosophila* males. Development 122, 1331–1341.
Love MI, Huber W, Anders S (2014). Moderated estimation of fold change and dispersion for RNA-seq data with DESeq2. Genome Biol 15, 550.
Mageeney CM, Kearse MG, Gershman BW, Pritchard CE, Colquhoun JM, Ware VC (2018). Functional interplay between ribosomal protein paralogues in the eRpL22 family in *Drosophila melanogaster*. Fly 12, 143–163.
Martin M (2011). Cutadapt removes adapter sequences from high-throughput sequencing reads. Bioinf Action 17, 10–12.
Marygold SJ, Roote J, Reuter G, Lambertsson A, Ashburner M, Millburn GH, Harrison PM, Yu Z, Kenmochi N, Kaufman TC, *et al*. (2007). The ribosomal protein genes and Minute loci of *Drosophila melanogaster*. Genome Biol 8, R216.
Mauro VP, Edelman GM (2002). The ribosome filter hypothesis. Proc Natl Acad Sci USA 19, 12031–12036.
McWilliam H, Li W, Uludag M, Squizzato S, Park YM, Buso N, Cowley AP, Lopez R (2013). Analysis Tool Web Services from the EMBL-EBI. Nucleic Acids Res 41, W597–W600.
Mi H, Huang X, Muruganujan A, Tang H, Mills C, Kang D, Thomas PD (2017). PANTHER version 11, expanded annotation data from Gene Ontology and Reactome pathways, and data analysis tool enhancements. Nucleic Acids Res 45, D183–D189.
Pircher A, Gebetsberger J, Polacek N (2014). Ribosome associated ncRNAs: An emerging class of translation regulators. RNA Biol 11, 1335–1339.
Qin X, Ahn S, Speed TP, Rubin GM (2007). Global analyses of mRNA translational control during early *Drosophila* embryogenesis. Genome Biol 8, R63.
Ramagopal S (1992). Are eukaryotic ribosomes heterogeneous? Affirmations on the horizon. Biochem Cell Biol 70, 269–272.
Schäfer M, Nayernia K, Engel W, Schäfer U (1995). Translational control in spermatogenesis. Dev Biol 172, 344–352.
Scott MS, Ono M (2011). From snoRNA to miRNA: dual function regulatory non-coding RNAs. Biochimie 93, 1987–1992.
Segev N, Gerst JE (2018). Specialized ribosomes and specific ribosomal protein paralogs control translation of mitochondrial proteins. J Cell Biol 217, 117–126.
Shi Z, Barna M (2015). Translating the genome in time and space: specialized ribosomes, RNA regulons, and RNA-binding proteins. Annu Rev Cell Dev Biol 31, 31–54.
Shi Z, Fujii K, Kovary KM, Genuth NR, Röst HL, Teruel MN, Barna M (2017). Heterogeneous ribosomes preferentially translate distinct subpools of mRNAs genome-wide. Mol Cell 67, 1–13.
Shigenobu S, Arita K, Kitadate Y, Noda C, Kobayashi S (2006a). Isolation of germ line cells from *Drosophila* embryos by flow cytometry. Dev Growth Differ 48, 49–57.
Shigenobu S, Kitadate Y, Noda C, Kobayashi S (2006b). Molecular characterization of embryonic gonads by gene expression profiling in *Drosophila melanogaster*. Proc Natl Acad Sci USA 103, 13728–13733.
Sievers F, Wilm A, Dineen DG, Gibson TJ, Karplus K, Li W, Lopez R, McWilliam H, Remmert M, Söding J, *et al*. (2011). Fast, scalable generation of high-quality protein multiple sequence alignments using Clustal Omega. Mol Syst Biol 7, 539.
Simsek D, Tiu GC, Flynn RA, Byeon GW, Leppek K, Xu AF, Chang HY, Barna M (2017). The mammalian ribo-interactome reveals ribosome functional diversity and heterogeneity. Cell 169, 1051–1065.e18.
Slavov N, Semrau S, Airoldi E, Budnik B, van Oudenaarden A (2015). Differential stoichiometry among core ribosomal proteins. Cell Rep 13, 865–873.
Tautz D, Hancock JM, Webb DA, Tautz C, Dover GA (1988). Complete sequences of the rRNA genes of *Drosophila melanogaster*. Mol Biol Evol 5, 366–376.
Wakimoto BT, Lindsley DL, Herrera C (2004). Toward a comprehensive genetic analysis of male fertility in *Drosophila melanogaster*. Genetics 167, 207–216.
Warner JR (1999). The economics of ribosome biosynthesis in yeast. Trends Biochem Sci 24, 437–440.
Warner JR, McIntosh KB (2009). How common are extraribosomal functions of ribosomal proteins? Mol Cell 34, 3–11.
Wasbrough ER, Dorus S, Hester S, Howard-Murkin J, Lilley K, Wilkin E, Polpitiya A, Petritis K, Karr TL (2010). The *Drosophila melanogaster* sperm proteome-II (DmSP-II). J Proteomics 73, 2171–2185.
Wen K, Yang L, Xiong T, Di C, MA D, Wu M, Xue Z, Zhang X, Long L, Zhang W, *et al*. (2016). Critical roles of long noncoding RNAs in *Drosophila* spermatogenesis. Genome Res 26, 1233–1244.
White-Cooper H (2010). Molecular mechanisms of gene regulation during *Drosophila* spermatogenesis. Reproduction 139, 11–21.
Wool IG (1996). Extraribosomal functions of ribosomal proteins. Trends Biochem Sci 21, 164–165.
Xue S, Barna M (2012). Specialized ribosomes: a new frontier in gene regulation and organismal biology. Nat Rev 13, 335–369.
Xue S, Tian S, Fujii K, Kladwang W, Das R, Barna M (2015). RNA regulons in Hox 5′ UTRs confer ribosome specificity to gene regulation. Nature 517, 33–38.
Zuker M (2003). Mfold web server for nucleic acid folding and hybridization prediction. Nucleic Acids Res 31, 3406–3415.